

# Northumbria Research Link

Citation: Erfanian Nakhchi Toosi, Mahdi and Rahmati, Mohammad (2021) Entropy Generation of Turbulent Cu-Water Nanofluid Flows inside Thermal Systems Equipped by Transverse-Cut Twisted turbulators. *Journal of Thermal Analysis and Calorimetry*, 143 (3). pp. 2475-2484. ISSN 1388-6150

Published by: Springer

URL: <https://doi.org/10.1007/s10973-020-09960-w> <<https://doi.org/10.1007/s10973-020-09960-w>>

This version was downloaded from Northumbria Research Link:  
<http://nrl.northumbria.ac.uk/id/eprint/43476/>

Northumbria University has developed Northumbria Research Link (NRL) to enable users to access the University's research output. Copyright © and moral rights for items on NRL are retained by the individual author(s) and/or other copyright owners. Single copies of full items can be reproduced, displayed or performed, and given to third parties in any format or medium for personal research or study, educational, or not-for-profit purposes without prior permission or charge, provided the authors, title and full bibliographic details are given, as well as a hyperlink and/or URL to the original metadata page. The content must not be changed in any way. Full items must not be sold commercially in any format or medium without formal permission of the copyright holder. The full policy is available online: <http://nrl.northumbria.ac.uk/policies.html>

This document may differ from the final, published version of the research and has been made available online in accordance with publisher policies. To read and/or cite from the published version of the research, please visit the publisher's website (a subscription may be required.)

# Entropy Generation of Turbulent Cu-Water Nanofluid Flows inside Thermal Systems Equipped by Transverse-Cut Twisted turbulators

M. E . Nakhchi<sup>a,1</sup>, M. T. Rahmati<sup>a</sup>

Faculty of Engineering and Environment, Northumbria University, Newcastle upon Tyne, NE1  
8ST, UK

## Abstract

In the present study, numerical simulations have been carried out on thermal characteristics and second law analysis of turbulent Cu-H<sub>2</sub>O nanofluid flow with the nanoparticle volume fraction of  $0 < \phi < 1.5\%$  inside heat exchangers fitted by transverse-cut twisted tapes (TCTTs) with alternates' axis. The transverse cut ratios are in the range of  $0.7 < b/c < 0.9$  and  $2 < s/c < 2.5$  and the Reynolds number is varied between 5000 and 15000. The impacts of the design variables on the turbulent kinetic energy, temperature distribution, thermal and frictional entropy generations, and Bejan number have been evaluated. The simulations show that the TCTTs with  $b/c=0.7$  generate higher turbulent kinetic energy compared to the  $b/c=0.9$  due to higher swirl generation and flow disturbance. The additional recirculating flow produced near the alternate edges is another main physical factor for heat transfer augmentation. It is found that raising the nanoparticles volume concentration reduces the thermal entropy generation which is attributed to the thermal conductivity enhancement of nanofluids. Besides, raising the nanoparticles volume concentration from 0 to 1.5% reduces the  $N_{g,thermal}$  by 23%.

*Keywords:* CFD, Entropy generation, Bejan number, Nanofluid, Thermal systems

---

<sup>1</sup> Corresponding author (Mahdi.nakhchi@northumbria.ac.uk)

## 1. Introduction

Thermal management is one of the most challenging tasks in the manufacturing of heat exchanger pipes and other thermal equipment such as solar systems, food industries, and refrigeration. Entropy generation analysis is essential in the design of thermal systems because the first law analysis of heat transfer of turbulent flows only considers energy conservation and it is not able to predict the available work and the destruct of the useful work in the thermal design of a system. Entropy generation examination is an essential aspect of the management of the thermohydraulic industries for performance optimization. Passive techniques are effective methods to improve the heat transfer rate inside heat exchangers without changing the primary geometry of them. Several passive strategies have been employed by researchers in the past years to intensify the heat transfer and thermal efficiency parameter of those systems, like twisted tapes [1-4], wavy and grooved surfaces [5-7], hollow cylinders [8], baffles [9], nanofluids [10-13] and twisted transverse baffles [14].

Twisted tapes are one of the most popular vortex generators in the design of thermal equipment because of their simple design and low manufacturing costs [1]. Twisted tapes can significantly improve the fluids mixing among the heat exchanger walls and the core. Several improved twisted tapes were employed in the past decade on thermohydraulic performance augmentation of heat exchanger equipment such as square-cut twisted tapes [15], twisted tape with perforations [16], twin twisted tapes [17], serrated Twisted tapes [18], short-length twisted tapes [19], delta-winglet twisted tapes [20], center-cleared twisted tape [21] and twisted tapes with alternates axis [22]. Eiamsa-ard et al. [23] experimentally evaluated the impacts of peripherally-cut twisted

tapes on the thermal efficiency of heat exchangers under laminar and turbulent flow conditions. They found that the Nusselt number could be around 2.6 times of that in the circular tubes without inserts. Hajabdollahi et al. [24] numerically examined the temperature distributions inside a fin and tube heat exchanger enhanced with twisted tapes. The outcome revealed that the twisted tape could significantly improve the heat transfer of the system compared to the circular ducts without turbulators under the same mass flow rates. They also performed a design optimization to maximize the efficiency of the heat exchangers tube by twisted tapes vortex generators.

Nanofluids have been widely employed as an efficient method for improving the thermophysical properties of working fluid by adding various nanoparticles [10, 25, 26]. Using nanoparticles can significantly augment the thermohydraulic performance of the heat exchanger system. Several researchers in the past few years suggested that a combination of nanofluids and twisted tape vortex generators can significantly improve the thermohydraulic efficiency of heat exchangers [27]. Twisted tapes could intensify the turbulent flow disturbance and flow severity between the tube surface and the central region, while the nanofluids could improve the thermophysical properties of the fluid. Maddah et al. [28] analyzed the effects of  $Al_2O_3$  nanoparticles on the thermohydraulic efficiency improvement of heat exchangers enhanced by geometrical progression ratio (GPR) TTs. They observed that of RGPR twisted tape together with nanofluids increase heat transfer rate by 12%.

Entropy generation analysis of thermal systems is very important in the design of heat transfer equipment and has obtained considerable attention in the past few years [29, 30]. In other words, entropy generation evaluation is a powerful technique to examine the performance of a thermal system. The systems with the least entropy generations could be taken into consideration as an

optimal system. Shamsabadi et al. [31] carried out a numerical study on the entropy generation of nanofluids flows inside a channel equipped by porous baffles. They found that raising the number of baffles from 4 to 16, decreases the thermal and frictional entropy generations by 14 and 32%, respectively. In another analytical research, Ellahi et al. [32] evaluated the impact of Cu nanoparticles shape on entropy generation of the MHD flows over vertical cone through numerical simulations. They concluded that the velocity of the fluid decreases by raising the nanoparticles volume fractions. They also revealed that increasing the diameter of the Cu nanoparticles could increase the entropy generation rate.

According to the literature survey, twisted tapes with cut edges can remarkably intensify the thermal performance of the heat exchangers compared to typical ones by increasing the fluid mixing and flow disturbance near the cuts. This kind of vortex generators has several industrial applications, mostly in boiling units of thermal power plans. However, there are no numerical or experimental investigations regarding the combined effects of nanofluids and transverse-cut twisted tapes to take advantage of both passive methods on thermal performance and entropy generation analysis. Moreover, entropy generation analysis needs to be provided to show the effects of the cut edges of the turbulators on the Bejan number, thermal and frictional entropy production of turbulent nanofluid flows in these systems. Entropy generation examinations could help to amend the thermal management of heat exchanger systems equipped with transverse-cut twisted tape.

## **2. Physical model**

Fig. 1 illustrates the schematics of the transverse-cut twisted tapes by alternates' axis inside a circular duct. The geometrical parameters are also presented. The tube length ( $L$ ) and diameter

( $D$ ) kept constant at 1100 mm and 20 mm. The width of the cuts ( $b$ ) and the depth of them ( $s$ ) are in the range of 14-18 mm and 40-50 mm, respectively. The dimensionless design parameters selected to investigate the effects of transverse-cut geometry on entropy generations are  $0.7 < b/c < 0.9$ , and  $2 < s/c < 2.5$ , in which  $c$  is the width of a typical TT, and it is equal to the tube diameter in the present study (Table 1). Six different transverse-cut twisted tapes were employed to examine the effects of Cu nanoparticles volume concentration and the design criterion in the thermal and frictional entropy generations in heat exchangers with the turbulent flow regime. The inlet velocity ( $u_i$ ) is kept identical and the Reynolds number ( $Re = u_i D / \nu$ ) is varied between 5,000 and 15,000. Constant wall heat flux is imposed on the tube walls in the current CFD study, and the Cu-water nanofluid inlet temperature ( $T_{in}$ ) is also assumed to be 300K.

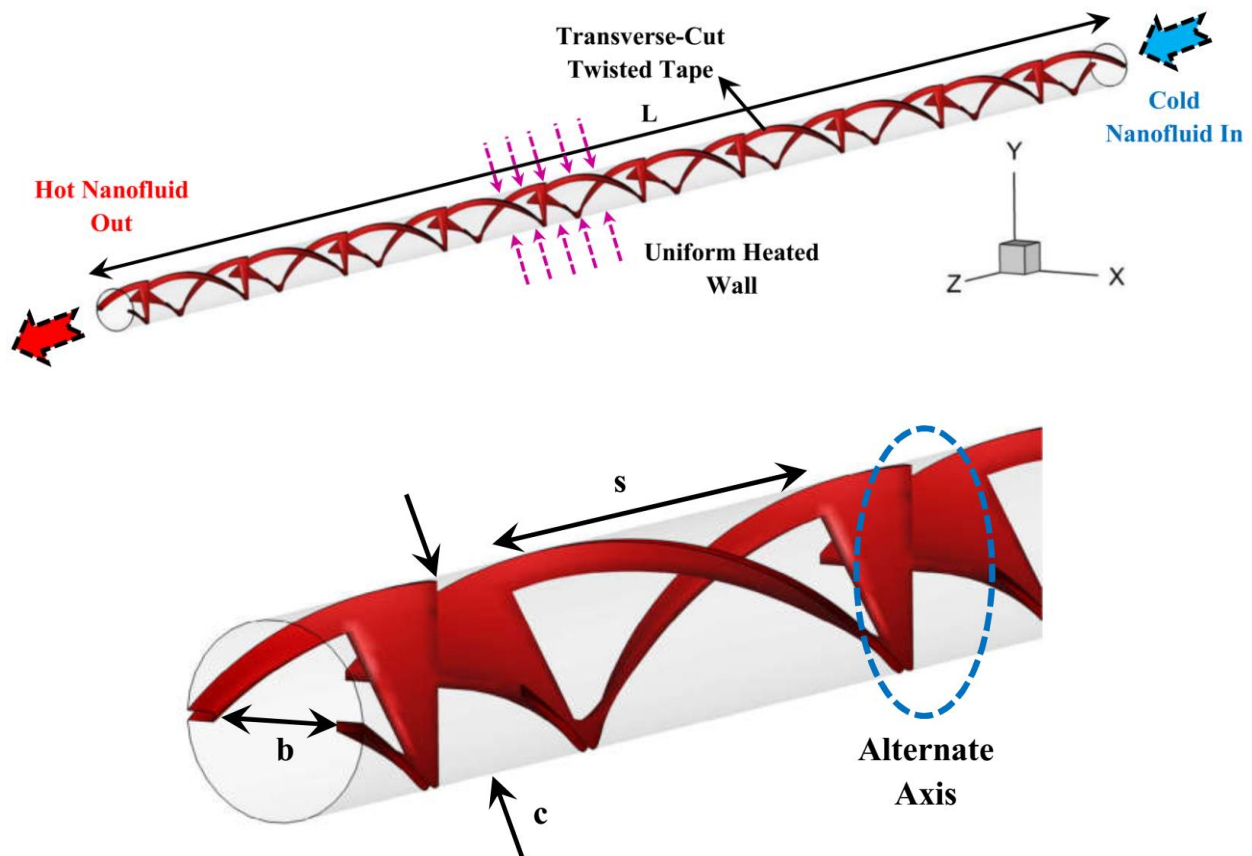


**Fig. 1** Schematic of heat exchanger enhanced by transverse-cut twisted tapes with alternating axes

**Table 1** Geometrical and physical parameters inside the pipe fitted with TCTT vortex generators

Parameter	Symbol	Value
Duct length	$(L)$	1100 mm
Duct diameter	$(D)$	20 mm
cut width	$(b)$	14-18 mm
Twist width	$(c)$	20 mm
Cut depth	$(s)$	40-50 mm
TCTT thickness	$(t)$	1 mm
Tube thickness	$(\delta)$	2 mm
TCTT width ratio	$b/c$	0.7-0.9
TCTT depth ratio	$s/c$	2-2.5
Reynolds number	Re	5,000-15000

### 3. Mathematical modeling

The partial differential equations of turbulent nano fluid flows for the present work are expressed by:

$$\frac{\partial}{\partial x_i} \langle ru_i \rangle = 0 \quad (1)$$

$$\frac{\partial}{\partial x_j} \langle u_j ru_i \rangle = - \frac{\partial p}{\partial x_i} + \frac{\partial}{\partial x_j} \left\langle - ru_i \overline{u_j} \right\rangle + \frac{\partial}{\partial x_j} \left\langle \frac{\partial}{\partial x_j} \left( \frac{\mu}{\rho} \left( \frac{\partial u_i}{\partial x_j} + \frac{\partial u_j}{\partial x_i} \right) \right) \right\rangle \quad (2)$$

$$\frac{\partial}{\partial x_j} \langle ru_i T \rangle = \frac{\partial}{\partial x_i} \left\langle \frac{m}{\rho} + \frac{m_t}{\rho_t} \right\rangle \frac{\partial T}{\partial x_i} \quad (3)$$

were  $\langle \overline{ru_i u_j} \rangle$  and  $(\mu_t)$  are expressed by:

$$\langle \overline{ru_i u_j} \rangle = m_t \frac{\partial u_i}{\partial x_j} + \frac{\mu_t}{\rho} \frac{\partial^2 u_j}{\partial x_i^2} - \frac{2}{3} r K d_{ij} - \frac{2}{3} m_t \frac{\partial u_k}{\partial x_k} d_{ij} \quad (4)$$

$$m_t = r C_m \frac{k^2}{\epsilon} \quad (5)$$

The RNG  $k-\epsilon$  model is a well-known model to predict the vortex generations of turbulent flows inside heat exchangers fitted by turbulators [33]. The governing transport equations are defined as:

$$\frac{\partial}{\partial x_i} (ru_i k) = \frac{\partial}{\partial x_j} \left( \frac{\mu_t}{s_k} \frac{\partial k}{\partial x_j} + m \right) + G_k - r \epsilon \quad (6)$$

$$\frac{\partial}{\partial x_i} (ru_i \epsilon) = \frac{\partial}{\partial x_j} \left( \frac{\mu_t}{s_\epsilon} \frac{\partial \epsilon}{\partial x_j} + m_\epsilon \right) + \frac{\epsilon}{k} [C_{1\epsilon} G_k - r C_{2\epsilon} \epsilon] \quad (7)$$

and  $G_k = \langle \overline{ru_i u_j} \rangle \frac{\partial u_j}{\partial x_i}$ . The constant coefficients of (RNG)  $k-\epsilon$  are  $s_\epsilon = 1.3$ ;  $C_{1\epsilon} = 1.42$ ;

$C_{2\epsilon} = 1.68$ ;  $C_m = 0.0845$ ;  $Pr_t = 0.85$  and  $s_k = 1$ .

The thermophysical properties of Copper-H<sub>2</sub>O nanofluids are evaluated by employing these correlations:

- Effective density:

$$\rho_{eff} = (1-\phi)\rho_f + \phi\rho_p \quad (8)$$

- Effective specific heat:



$$C_{eff} = \frac{(1-\phi)\rho_f C_f + \phi\rho_p C_p}{\rho_{eff}} \quad (9)$$

- Effective viscosity [34]:

$$\mu_{eff} = \frac{\mu_f}{(1-\phi)^{2.5}} \quad (10)$$

- Effective thermal conductivity [35]:

$$\frac{k_{eff}}{k_f} = \frac{k_p + 2k_f + 2\phi(k_p - k_f)}{k_p + 2k_f - \phi(k_p - k_f)} \quad (11)$$

where  $\phi$ ,  $f$ ,  $p$  and  $eff$  are volume concentration of nano particles, main fluid (H<sub>2</sub>O), particles, and effective nano fluid, respectively. The thermophysical properties of Cu nanoparticles based on the average diameter of 50 nm are  $\rho_p = 8300 \text{ kg m}^{-3}$ ,  $C_p = 420 \text{ J kg}^{-1} \text{ K}^{-1}$  and  $k_p = 401 \text{ W m}^{-1} \text{ K}^{-1}$ . The volume concentration of nano particles is between 0% and 1.5% in the present numerical simulations.

The local volumetric entropy generations, considered for thermal and frictional impacts are expressed by [36]:

$$S_{g,th}'' = \left( \frac{k + k_t}{T^2} \right) \left[ \left( \frac{\partial T}{\partial x} \right)^2 + \left( \frac{\partial T}{\partial y} \right)^2 + \left( \frac{\partial T}{\partial z} \right)^2 \right] \quad (12)$$

$$S_{g,p}'' = \left( \frac{\mu + \mu_t}{T} \right) \left\{ 2 \left[ \left( \frac{\partial u}{\partial x} \right)^2 + \left( \frac{\partial v}{\partial y} \right)^2 + \left( \frac{\partial w}{\partial z} \right)^2 \right] + \left( \frac{\partial u}{\partial y} + \frac{\partial v}{\partial x} \right)^2 + \left( \frac{\partial u}{\partial z} + \frac{\partial w}{\partial x} \right)^2 + \left( \frac{\partial v}{\partial z} + \frac{\partial w}{\partial y} \right)^2 \right\} \quad (13)$$

and  $u$ ,  $v$  and  $w$  were accounted for velocity vectors in different directions, respectively.  $\mu_t$  denotes turbulence viscosity and  $k_t$  attributes the thermal conductivity. The above formulations may be converted to the dimensionless forms of entropy production with employing these formulations:

$$N_{g,thermal} = \frac{S_{g,th}''' D_h^2}{k} \quad (14)$$

$$N_{g,viscous} = \frac{S_{g,p}''' D_h^2}{k} \quad (15)$$

The Bejan number is expressed by:

$$Be = \frac{S_{g,thermal}'''}{S_{g,thermal}''' + S_{g,viscous}'''} \quad (16)$$

### 3.1. Mesh generation

Ansys ICEM 19.3 is utilized for mesh generation inside the heat exchanger pipe enhanced by transverse-cut TT insert. Fig. 2 depicts the mesh used in the present numerical simulations. As can be observed, the mesh is generated based on the non-uniform adaptive method and smaller mesh size is employed near the cut edges to measure the turbulent kinetic energy and severity disturbance in these regions.

The detailed view of the tube inlet mesh illustrates that the inflated grid is employed near the pipe walls ensuring that  $y^+$  values are kept less than one in the whole body to resolve the sub-layer effects near the boundaries under turbulent flow regime. The finite volume method is employed to resolve the 3D Navier-Stokes governing equations. The second order upwind

scheme is utilized for the discretization of the mathematical equations. The residuals of the Eqs. (1-3) are recorded to confirm that the convergence of computations, in which the convergence criteria is assumed to be  $10^{-7}$ . Ansys Fluent 19.3 is utilized for the computations and the SIMPLE algorithm is used for pressure--velocity couplings.

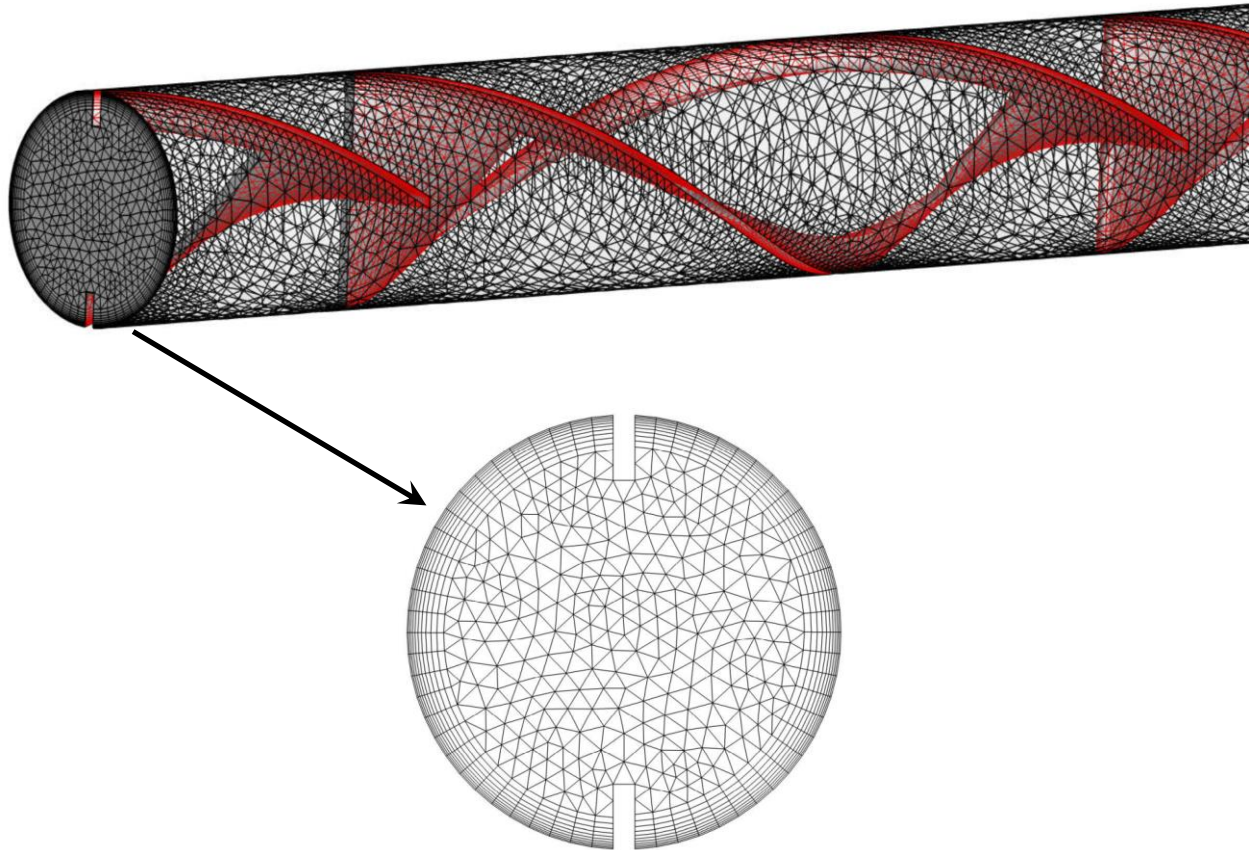


**Fig. 2** Mesh generation through heat exchanger pipe enhanced by Transverse-cut TTs with alternating axes and the detailed view of the inlet

Table 2 displays the grid independency test performed for the average Nusselt number ( $Nu = hD / k_{nf}$ ) of turbulent Cu-water nanofluids ( $\phi = 1.5\%$ ) flows through the heat exchanger duct equipped by transverse-cut TTs by alternating axis with  $b/c=0.7$  and  $s/c=2$  at  $Re=15000$  (extreme case). Four different grid numbers (506221, 925380, 1412903 and 2103556 elements)

were selected to perform the CFD calculations. It can be seen that the deviation between 1412903 and 2103556 elements is around 0.3%. Therefore, 1412903 grid numbers are selected for further calculations.

**Table 2** Grid independence study for  $b/c=0.7$  and  $s/c=2$  at  $Re = 15,000$  and  $\phi = 1.5\%$  .

Element number	$Nu$	Dev. %
506221	186.91	-
925380	200.42	7.2
1412903	208.67	4.1
2103556	209.20	0.3

### 3.2. Validation of numerical results

Before further simulations, it is necessary to check the accuracy of the present turbulent model used for the numerical simulations. Several turbulent models ( $k-\varepsilon$ ,  $k-\omega$ , SST- $k-\omega$ , and Renormalization Group  $k-\varepsilon$  models) were utilized and the outputs of each model were validated with the empirical data existing in the previous studies. Among the turbulent models, the RNG  $k-\varepsilon$  model has more accurate results compared with the experimental data. For this purpose, the numerical results of turbulent flows inside channels fitted by typical twisted tape inserts are validated with the experimental data of Manglik and Bergles [37] for turbulent flow heat transfer in heat exchangers inserted by conventional TTs without cut edges in Fig. 3. The comparison illustrates that the numerical results of the current study match well with the experimental results. Consequently, RNG  $k-\omega$  model is utilized for further computations. It is seen that the  $Nu$

number enhances by raising the Re number that is attributed to the stronger velocity gradients of turbulent flow at higher Re numbers.

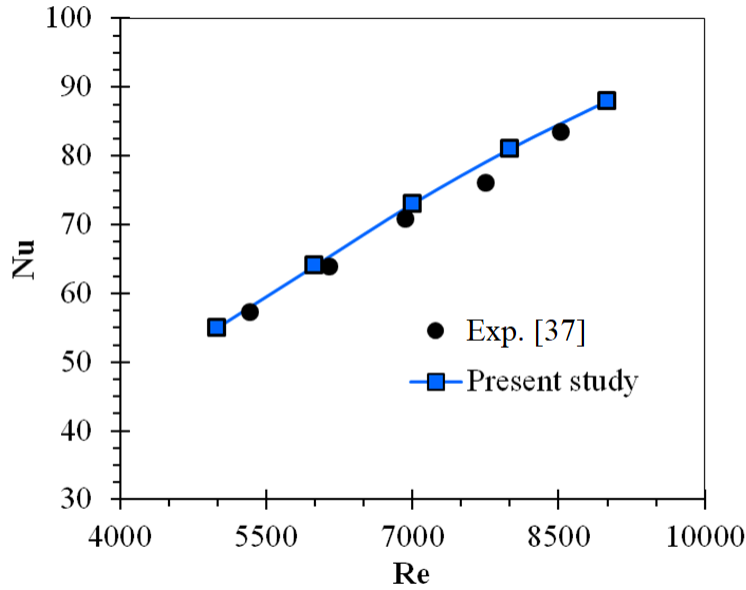


**Fig. 3** Validating of numerical calculations with experiments of Manglik and Bergles [37] for conventional twisted tapes

It also should be pointed out that additional checks were also performed to validate the accuracy of the selected turbulence model with nanofluids with respect to experimental data. The details of the validations for various Reynolds numbers can be found in [38].

#### 4. Results and discussion

Fig. 4 depicts the turbulent flow streamlines of nanofluid flows in a plain pipe and a duct equipped by TCTTs with an alternating axis. The flow streamlines are plotted as functions of the turbulent kinetic energy (TKE). The results demonstrate that TCTT significantly intensifies the flow severity between the pipe wall and the core areas. The primary advantage of this type of modified twisted tape compared to typical ones is that the cut area could considerably increase

the flow perturbations and the mixing of hot and cold flows between the pipe surfaces and the core area. It is also observed that the turbulent kinetic energy near the alternate axis is greater than the other regions. The alternate axis of the twisted tape changes the swirl flow direction and intensifies the turbulent kinetic energy in this area.

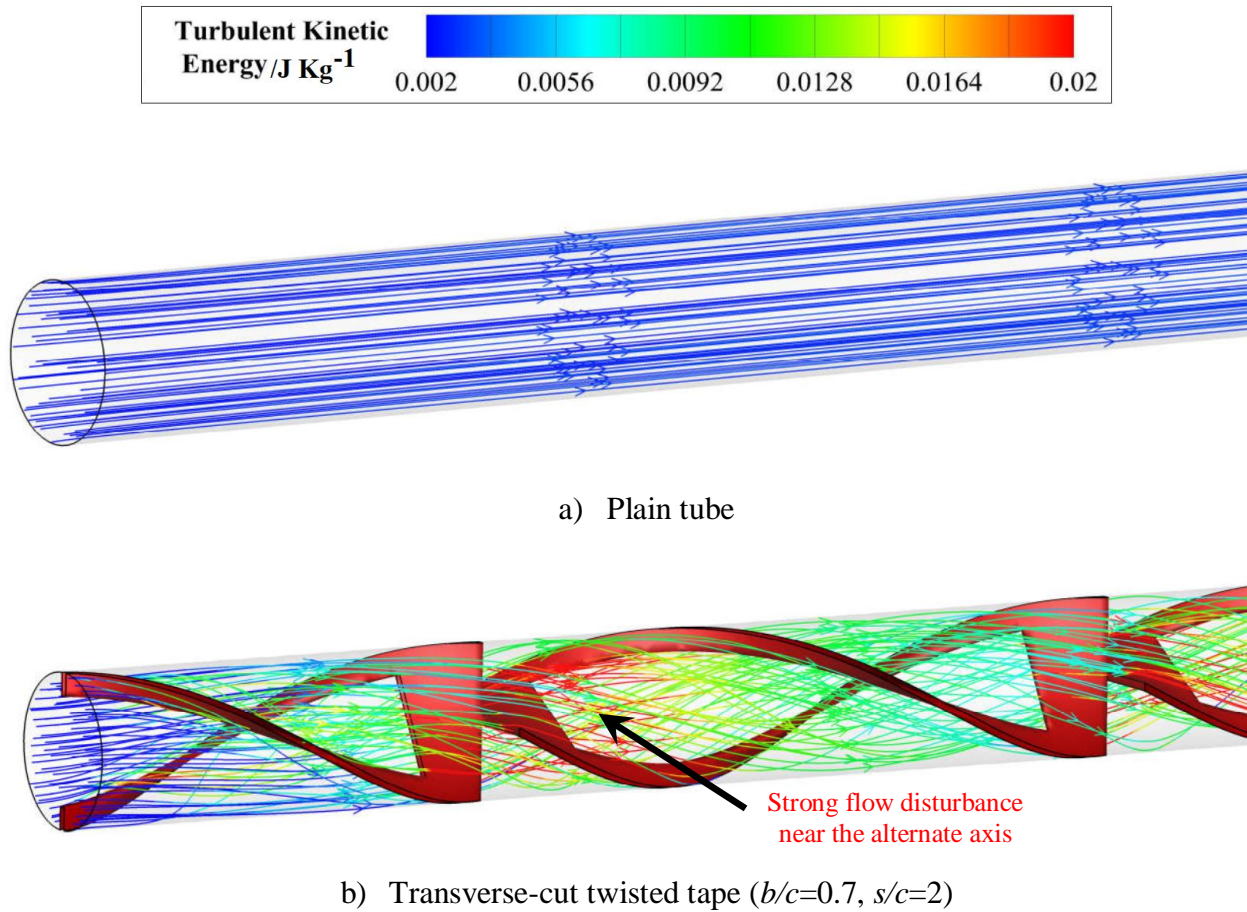


**Fig. 4** Streamlines of turbulent nanofluids flow ( $\phi = 0.5\%$ ) in the plain pipe and the pipe fitted by TC twisted tape ( $Re=9,000$ ,  $s/c=2$ ,  $b/c=0.7$ )

Fig. 5 illustrates the cross-section views of turbulent kinetic energy contours of nanofluids current inside heat exchangers enhanced by TCTTs with two different b/w ratios. The results show that the TTs with  $b/c=0.7$  generate higher turbulent kinetic energy compared to the  $b/c=0.9$  case. Physically speaking, using transverse-cut TCTTs with thicker cut edges ( $b/c=0.7$ ) are able

to generate stronger swirl flow and flow disturbance compared to the modified TTs by thin edges ( $b/w=0.9$ ). As depicted below, for both cases, the rate of TKE significantly increases near the alternate axis junction. The alternate axis creates secondary flows in the form of additional vortex flows.

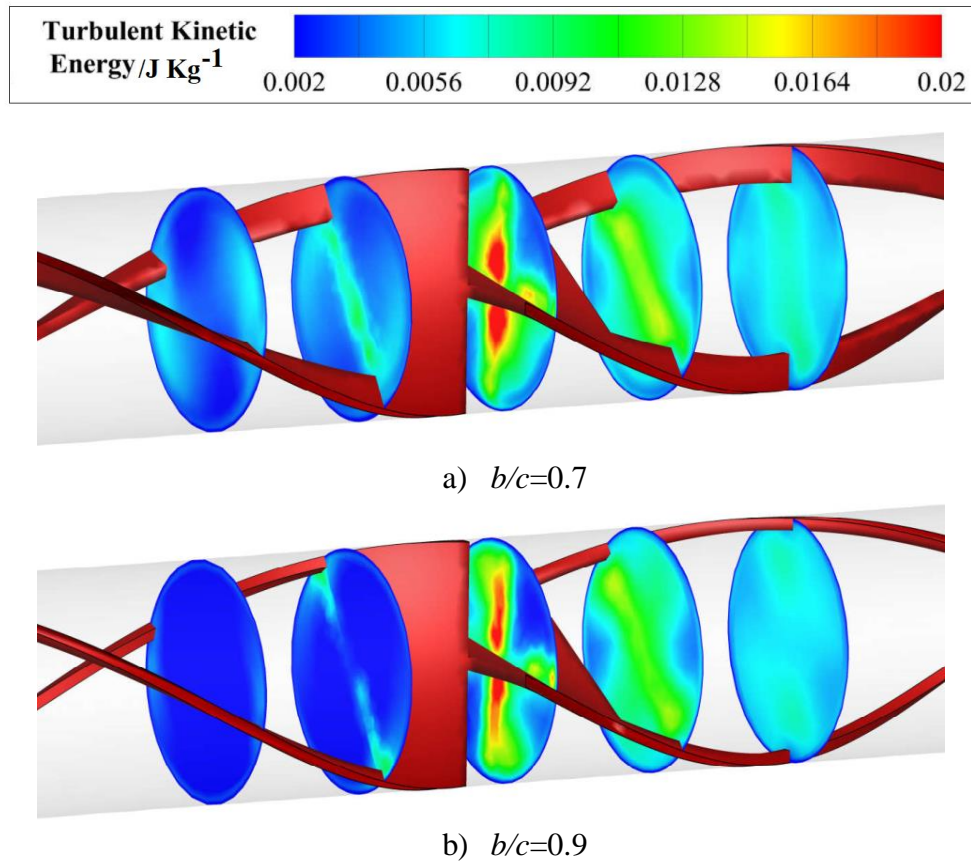


**Fig. 5** Kinetic energy contour plot of turbulence flows through tubes fitted by TC twisted tapes with an alternate axis ( $Re=9,000$ ,  $s/c=2$ ,  $\phi = 0.5\%$  )

Fig. 6 depicts the influence of TCTT geometry on the temperature distributions of turbulent Cu-water nanofluids flow through heat exchangers. The Re number is constant (9,000) and the Cu nano particles volume fraction is 0.5%. The results show that the TC twisted tapes with smaller width ratios ( $b/c$ ) have better heat transfer and the temperature of nanofluid enhances faster than of the cases with larger width ratios ( $b/c=0.9$ ). Generally, twisted tapes thicker edges generate



stronger flow disturbance due to the higher number of twists. It also can be seen that temperature augmentation near the alternate axis is strong for all of the test cases. As discussed earlier, the additional recirculating flows produced near the alternate edges, is the primary physical factor for heat transfer intensification.

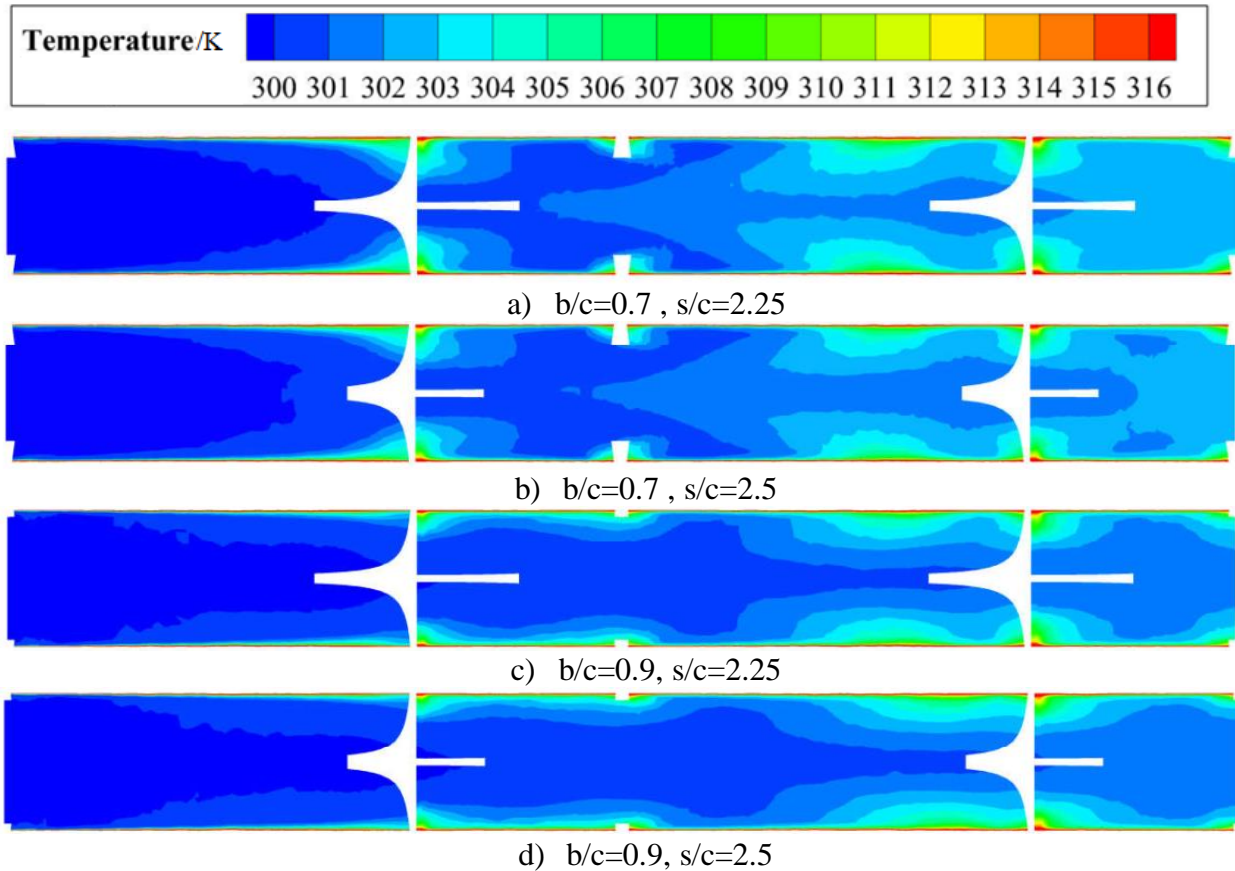
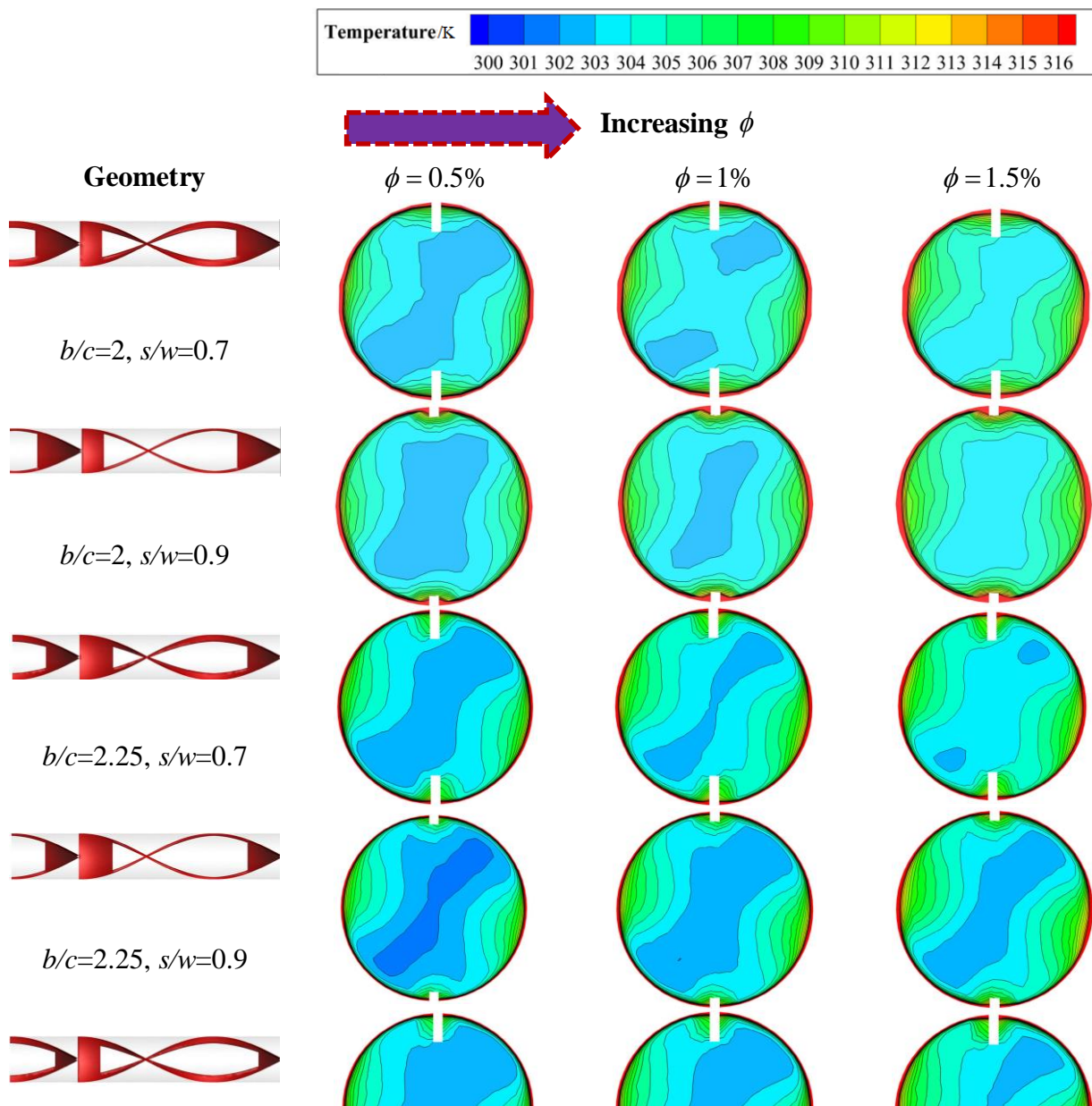


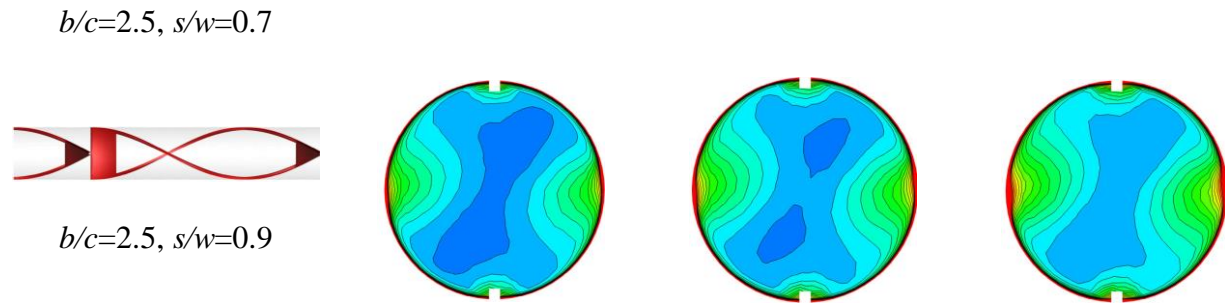
**Fig. 6** Temperature distribution of nanofluid flow inside tubes fitted by transverse-cut twisted tapes with various geometries at  $Re=9,000$ ,  $\phi = 0.5\%$ .

The effect of Cu nanoparticles on the temperature enhancement of turbulent nanofluids flow in heat exchangers with T-C twisted tapes with various cut ratios and cut ratios are presented in Fig. 7. The cross-section contours are plotted at  $z=0.18m$  and the nanoparticles volume concentration is changed from 0% (pure water) to 1.5%. The results show that the temperature of nanofluid



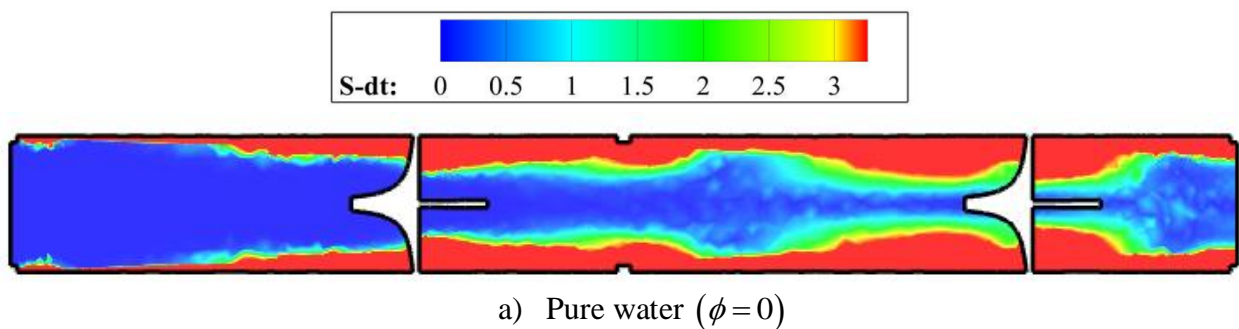
flow enhances by increasing  $\phi$ . The most important physical reason for temperature augmentation by adding Cu nanoparticle additives to the base fluid is that the thermophysical properties of the working fluid can considerably be improved by increasing  $\phi$  (see Eqs. 9-12). It also can be deduced that the temperature enhancement for  $b/c=2$ ,  $s/w=0.7$  is better than the other geometries. As discussed in Fig. 5, TCTTs with thicker width intensify the turbulent kinetic energy production due to stronger flow disturbance near the cut edges.

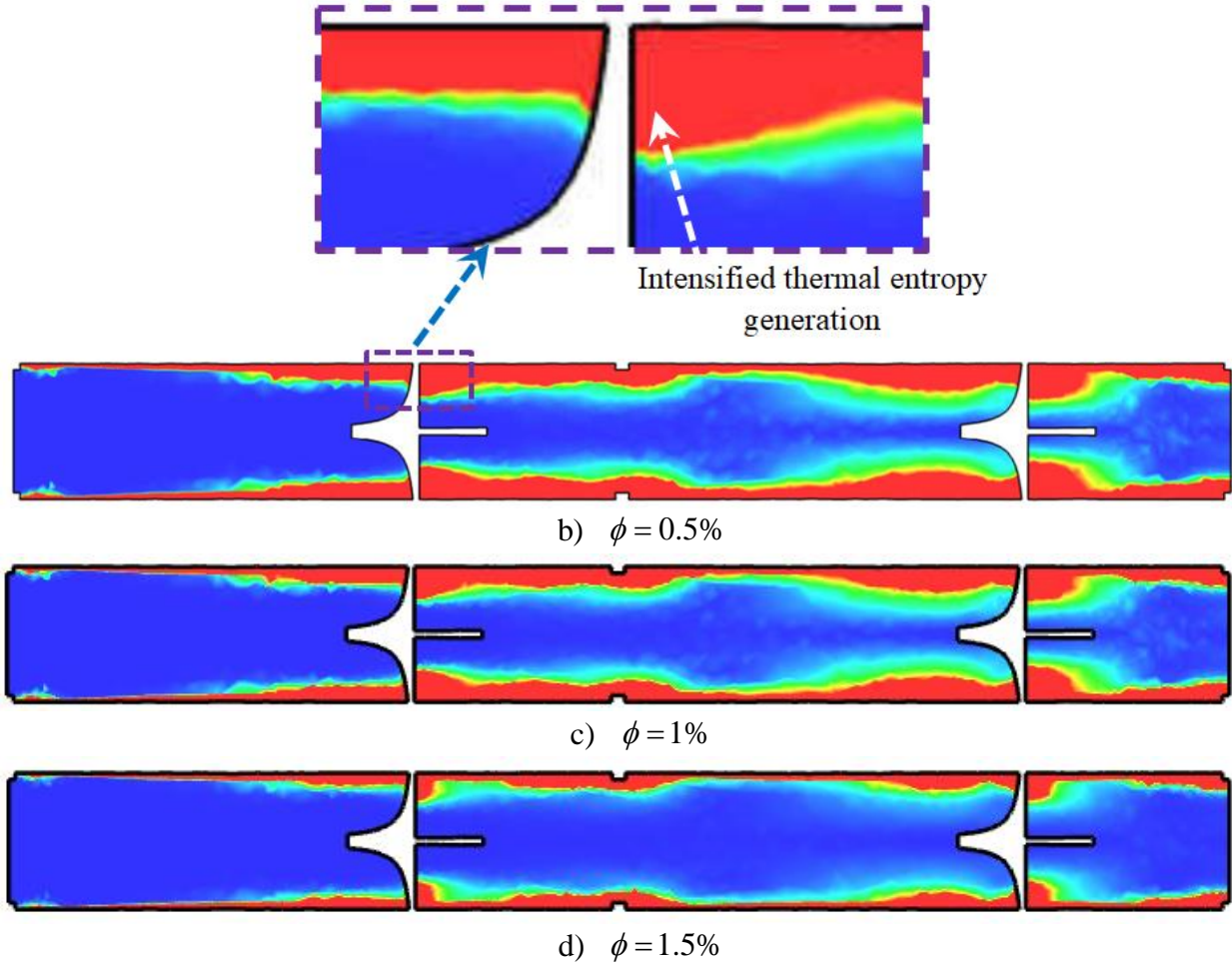




**Fig. 7** The effects of cut ratios and nanoparticles volume fraction of temperature distribution inside heat exchangers fitted by TCTT ( $Re = 9,000$ )

Fig. 8 displays the thermal entropy generations of nanofluids flows inside heat exchangers equipped by TC twisted tapes with various nanoparticle volume fraction. According to the description of the thermal entropy generation (Eq. 13), temperature gradients are the main reason for the augmentation of this parameter. The results show that the rate of thermic entropy production near the pipe surface is much higher in comparison with the tube center for all of the cases. Strong recirculation flow near the tube walls in the existence of TTs interrupts the thermal B-L and the temperatures gradient increases. In addition, the alternate axis of the TC twisted tape generates strong swirl flow in those regions and intensifies the thermal entropy generation. It also can be seen that increasing the nanoparticles volume fraction reduces the thermal entropy production. This reduction is attributed to the thermal conductivity augmentation of nanofluids that improves the thermal performance and decreases the dissipations.

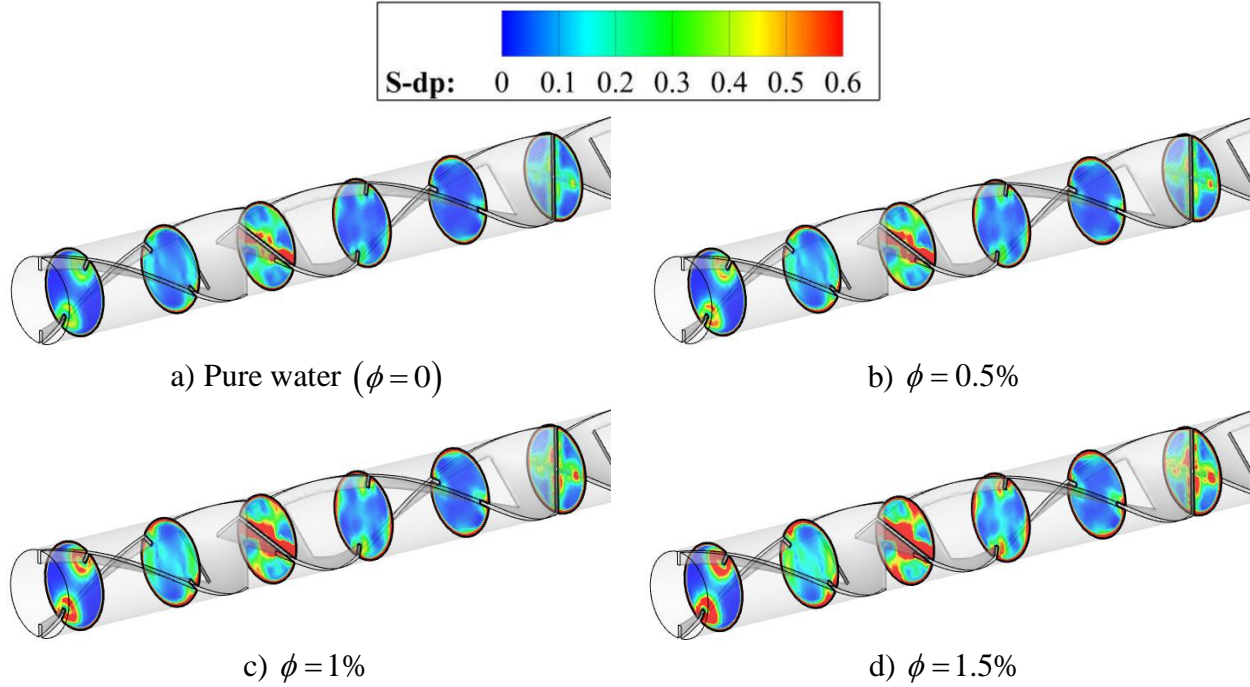




**Fig. 8** Thermal entropy generations of nanofluid flows inside heat exchangers enhanced by TC twisted tapes with  $b/c=0.9$  and  $s/c=2.25$ .

The impacts of Cu nano particles volume concentration on the frictional entropy production of turbulent flows inside the tubes enhanced by transverse-cut twisting tapes with  $b/c=0.7$  and  $s/c=2.25$  at  $Re=9,000$  are depicted in Fig. 9. The results are presented at six different cross-sections. It is noticed that the viscous entropy production significantly increases near the alternate axis of the TC twisted tape. The main physical reason for this augmentation is strong turbulent velocity gradients in this region generated by the sudden change in the swirl flow direction. It is observed that raising the nanoparticles volume concentration increases the frictional entropy production. As the volume fraction of the nanoparticles ( $\phi$ ) is improved, the

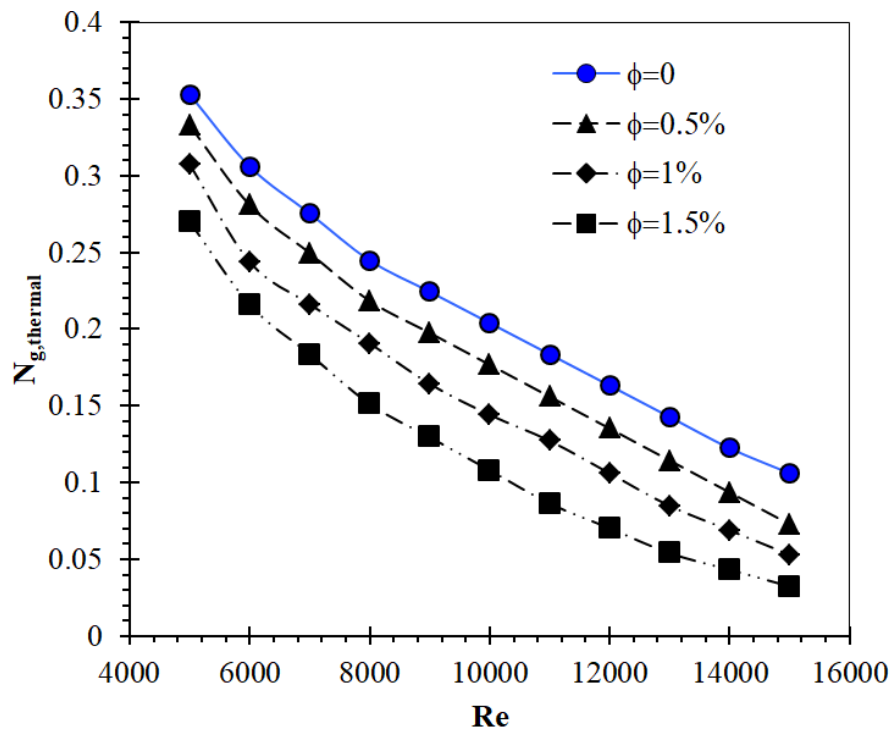
fluid velocity must be increased to keep the Re number constant. Therefore, the frictional entropy generation goes up. Besides, the viscosity of the nanofluid goes up by raising  $\phi$ . As a consequence, the frictional (viscous) entropy production increases (see Eq. 14)



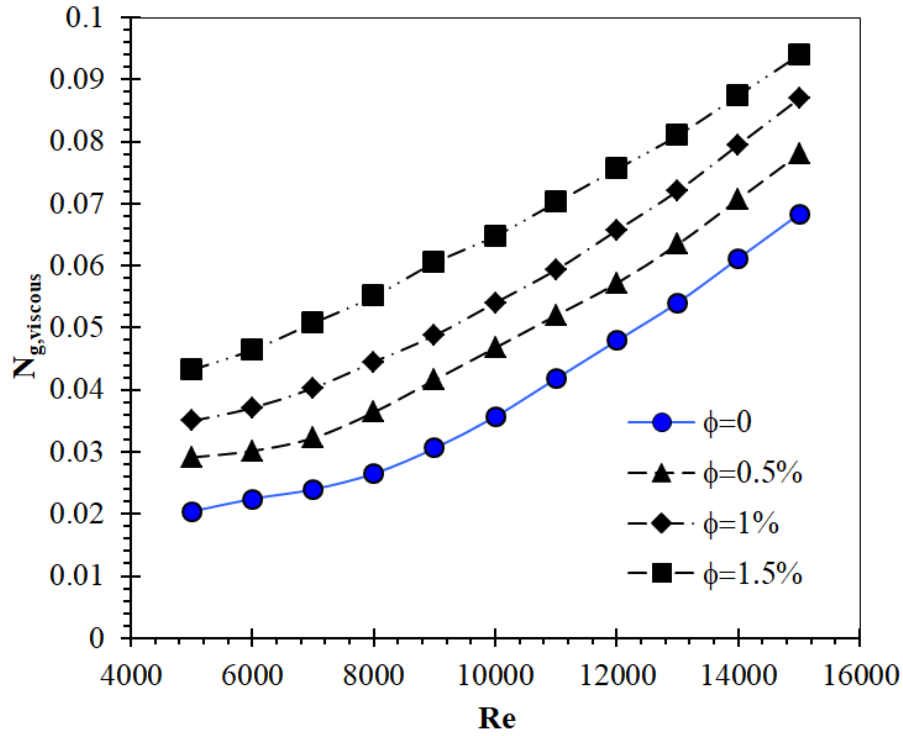
**Fig. 9** Viscous entropy production contour plots of nanofluids flow in heat exchangers fitted by TCTTs with  $b/c=0.9$  and  $s/c=2.25$ .

Fig. 10 depicts the dimensionless entropy generation of turbulent nanofluid flows inside heat exchanger pipes fitted by TCTTs with ( $b/c=0.7$  and  $s/c=2.25$ ) at various Re numbers. The results show that the thermal entropy production decreases by raising the Reynolds number from 5,000 to 15000. Physically speaking, the heat transfer rates augment with raising the Re number which means that the rate of thermal dissipations would be decreased. In addition, increasing the nanoparticles volume concentration from 0 to 1.5% reduces the  $N_{g,thermal}$  around 23% at  $Re=5,000$ . As discussed earlier, increasing the Cu nanoparticles  $\phi$  improves the thermal conductivity and other thermophysical properties of working fluid and improves the heat transfer

rate (entropy production reduction). As presented in Fig. 10-b viscous entropy production rises with raising the Reynolds number. The frictional entropy generations are depending on the velocity gradients. As the Reynolds number rises, the velocity gradients of nanofluid flow go up and the frictional entropy generation augments. It also can be deduced that the  $N_{g,viscous}$  enhances around 57% as the Cu nanoparticles volume concentration is raised from 0 to 1.5%.



a) Dimensionless thermal entropy generation



b) Dimensionless viscous entropy generation

**Fig. 10** Effects of the nanoparticle volume concentration on thermal and viscous entropy production

Fig. 11 shows the contours of Bejan number inside heat exchanger tubes equipped by transverse-cut twisted tapes with various cut ratios. It can be observed that the frictional entropy production at the inlet of the tube is dominant for all of the test cases. Physically speaking, at the hydraulic entry region of the heat exchangers, the velocity gradients are high and as a consequence, the viscous entropy production intensifies. However, after passing the entrance area, the thermal entropy generation becomes dominant, and the Bejan number tends to unity. This indicates that the temperature gradients due to the strong swirl generation near the TCTTs can significantly increase the generation of thermal entropy in these areas. The results illustrate that the Bejan number for the  $b/c=0.7$  is generally superior to  $b/c=0.9$  cases. This means that the transverse-cut twisted tapes with thicker cut edges can produce more intense vortex generations.



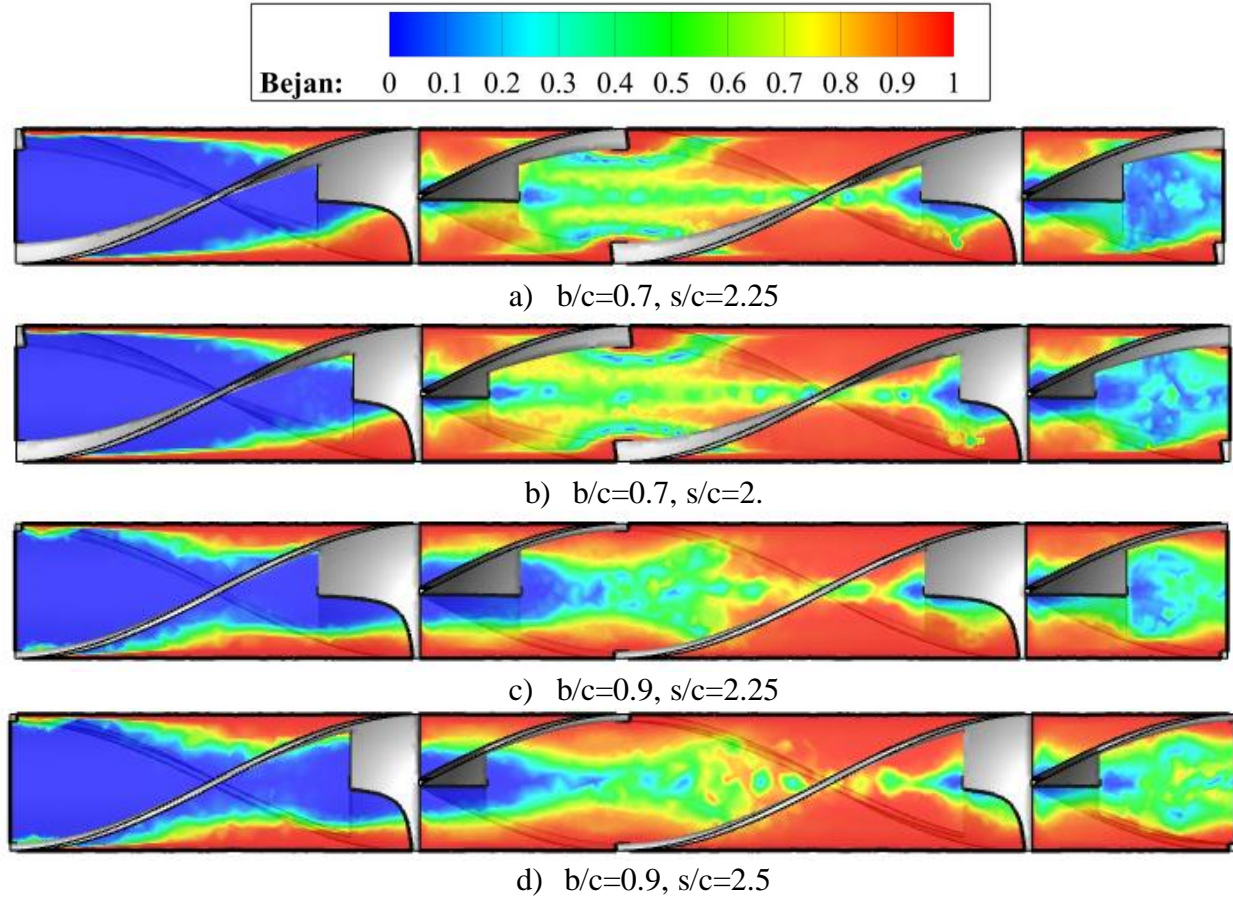


**Fig. 11** Bejan number contours of nanofluid flows in heat exchangers equipped by TC twisted tapes with  $Re=15,000$ .

Fig. 12 displays the impacts of nano particles volume fractions on the Bejan number values inside the heat exchangers fitted by TCTTs with  $b/c=0.7$  and  $s/c=2$ . The Cu nanoparticles volume fraction is between 0 and 1.5% and the Reynolds number is maintained at  $Re=15,000$ . It can be seen that the Bejan number slightly decreases with increasing  $\phi$ . Based on the definition of this parameter, it means that the effects of the nanoparticle volume concentration on frictional entropy production ( $S'''_{viscous}$ ) are higher than that on thermal entropy generation ( $S'''_{thermal}$ ). The cross-section contours illustrate that the viscous entropy generations near the alternate axis (blue color contours) is higher than the other regions. This indicates that the strong flow disturbance

and vortex generation due to the sudden turn at the junction of the TTs is the primary reason for friction factor augmentation due to the strong velocity gradients.

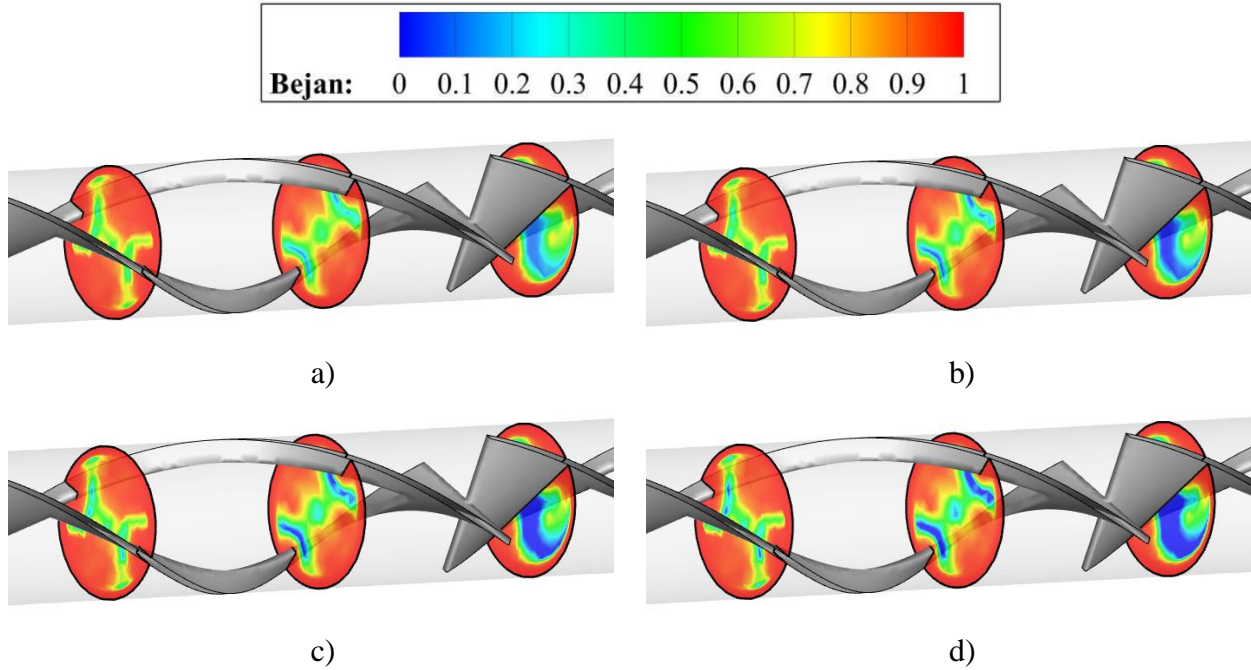


**Fig. 12** The impacts of nanoparticles volume concentration on the Bejan number contours

## 5. Conclusion

The impacts of transverse-cut twisted tapes on the thermal characteristics and entropy production analysis of Cu-water nanofluids flow inside heat exchangers with uniform wall heat flux were numerically investigated. The Reynolds number, cut width ratio, cut depth ratio and nanoparticles volume fraction were between  $5000 < Re < 15000$ ,  $0.7 < b/c < 0.9$ ,  $2.0 < s/c < 2.5$  and  $0 < \phi < 1.5\%$ , respectively. The most important conclusions of the present work are as follows:

- Transverse-cut twisted tapes with thicker cut edges ( $b/c=0.7$ ) can generate stronger swirl flow and flow disturbance compared to the modified TTs with thin margins ( $b/w=0.9$ ). The rate of TKE also significantly increases near the alternate axis junction.



- The rate of thermic entropy production near the pipe surface is much higher in comparison with the tube center for all of the cases. Strong recirculation flow near the tube walls in the existence of TTs interrupts the thermal B-L and the temperatures gradient increases.
- Increasing the nanoparticles volume concentration from 0 to 1.5% reduces the  $N_{g,thermal}$  around 23% at Re=5,000.
- $N_{g,viscous}$  rises up to 57% as the Cu nanoparticles volume concentration increases from 0% to 1.5%, while  $N_{g,thermal}$  reduces around 23% with similar conditions.
- At the entry region of the heat exchangers, the velocity gradients are high and as a result, the viscous entropy generation intensifies.

## References

1. Hosseinejad R, Hosseini M, Farhadi M. Turbulent heat transfer in tubular heat exchangers with twisted tape. *Journal of Thermal Analysis and Calorimetry*. 2019;135(3):1863-9.
2. Singh SK, Sarkar J. Improving hydrothermal performance of double-tube heat exchanger with modified twisted tape inserts using hybrid nanofluid. *Journal of Thermal Analysis and Calorimetry*. 2020:1-12.
3. Nakhchi ME, Esfahani J. Sensitivity analysis of a heat exchanger tube fitted with cross-cut twisted tape with alternate axis. *Journal of Heat Transfer*. 2019;141(4):041902.
4. Noorbakhsh M, Zaboli M, Ajarostaghi SSM. Numerical evaluation of the effect of using twisted tapes as turbulator with various geometries in both sides of a double-pipe heat exchanger. *Journal of Thermal Analysis and Calorimetry*. 2019:1-13.

5. Zhou J, Hatami M, Song D, Jing D. Design of microchannel heat sink with wavy channel and its time-efficient optimization with combined RSM and FVM methods. *International Journal of Heat and Mass Transfer*. 2016;103:715-24.
6. Nouri-Borujerdi A, Nakhchi M. Prediction of local shear stress and heat transfer between internal rotating cylinder and longitudinal cavities on stationary cylinder with various shapes. *International Journal of Thermal Sciences*. 2019;138:512-20.
7. Mosayebidorcheh S, Hatami M. Analytical investigation of peristaltic nanofluid flow and heat transfer in an asymmetric wavy wall channel (Part II: Divergent channel). *International Journal of Heat and Mass Transfer*. 2018;126:800-8.
8. Nakhchi M, Esfahani J. Numerical investigation of heat transfer enhancement inside heat exchanger tubes fitted with perforated hollow cylinders. *International Journal of Thermal Sciences*. 2020;147:106153.
9. Ghanbari S, Javaherdeh K. Investigation of applying nanoporous graphene non-Newtonian nanofluid on rheological properties and thermal performance in a turbulent annular flow with perforated baffles. *Journal of Thermal Analysis and Calorimetry*. 2020;139(1):629-47.
10. Akbarzadeh M, Rashidi S, Karimi N, Ellahi R. Convection of heat and thermodynamic irreversibilities in two-phase, turbulent nanofluid flows in solar heaters by corrugated absorber plates. *Advanced Powder Technology*. 2018;29(9):2243-54.
11. Ellahi R, Tariq MH, Hassan M, Vafai K. On boundary layer nano-ferroliquid flow under the influence of low oscillating stretchable rotating disk. *Journal of Molecular Liquids*. 2017;229:339-45.

12. Hatami M, Zhou J, Geng J, Song D, Jing D. Optimization of a lid-driven T-shaped porous cavity to improve the nanofluids mixed convection heat transfer. *Journal of Molecular Liquids*. 2017;231:620-31.
13. Zheng Y, Yang H, Mazaheri H, Aghaei A, Mokhtari N, Afrand M. An investigation on the influence of the shape of the vortex generator on fluid flow and turbulent heat transfer of hybrid nanofluid in a channel. *Journal of Thermal Analysis and Calorimetry*. 2020:1-14.
14. Rashidi S, Akbarzadeh M, Karimi N, Masoodi R. Combined effects of nanofluid and transverse twisted-baffles on the flow structures, heat transfer and irreversibilities inside a square duct—a numerical study. *Applied Thermal Engineering*. 2018;130:135-48.
15. Saravanan A, Senthilkumar J, Jaisankar S. Performance assessment in V-trough solar water heater fitted with square and V-cut twisted tape inserts. *Applied Thermal Engineering*. 2016;102:476-86.
16. Suri ARS, Kumar A, Maithani R. Heat transfer enhancement of heat exchanger tube with multiple square perforated twisted tape inserts: experimental investigation and correlation development. *Chemical Engineering and Processing: Process Intensification*. 2017;116:76-96.
17. Bahiraei M, Mazaheri N, Hassanzamani SM. Efficacy of a new graphene–platinum nanofluid in tubes fitted with single and twin twisted tapes regarding counter and co-swirling flows for efficient use of energy. *International Journal of Mechanical Sciences*. 2019;150:290-303.
18. Eiamsa-Ard S, Promvong P. Thermal characteristics in round tube fitted with serrated twisted tape. *Applied Thermal Engineering*. 2010;30(13):1673-82.
19. Eiamsa-Ard S, Thianpong C, Eiamsa-Ard P, Promvong P. Convective heat transfer in a circular tube with short-length twisted tape insert. *International communications in heat and mass transfer*. 2009;36(4):365-71.

20. Eiamsa-Ard S, Wongcharee K, Eiamsa-Ard P, Thianpong C. Heat transfer enhancement in a tube using delta-winglet twisted tape inserts. *Applied Thermal Engineering*. 2010;30(4):310-8.
21. Guo J, Fan A, Zhang X, Liu W. A numerical study on heat transfer and friction factor characteristics of laminar flow in a circular tube fitted with center-cleared twisted tape. *International Journal of Thermal Sciences*. 2011;50(7):1263-70.
22. Eiamsa-Ard S, Somkleang P, Nuntadusit C, Thianpong C. Heat transfer enhancement in tube by inserting uniform/non-uniform twisted-tapes with alternate axes: Effect of rotated-axis length. *Applied Thermal Engineering*. 2013;54(1):289-309.
23. Eiamsa-ard S, Seemawute P, Wongcharee K. Influences of peripherally-cut twisted tape insert on heat transfer and thermal performance characteristics in laminar and turbulent tube flows. *Experimental Thermal and Fluid Science*. 2010;34(6):711-9.
24. Hajabdollahi Z, Hajabdollahi H, Kim KC. Heat transfer enhancement and optimization of a tube fitted with twisted tape in a fin-and-tube heat exchanger. *Journal of Thermal Analysis and Calorimetry*. 2019:1-13.
25. Ellahi R, Zeeshan A, Shehzad N, Alamri SZ. Structural impact of kerosene-Al<sub>2</sub>O<sub>3</sub> nanoliquid on MHD Poiseuille flow with variable thermal conductivity: Application of cooling process. *Journal of Molecular Liquids*. 2018.
26. Esfahani J, Akbarzadeh M, Rashidi S, Rosen M, Ellahi R. Influences of wavy wall and nanoparticles on entropy generation over heat exchanger plat. *International Journal of Heat and Mass Transfer*. 2017;109:1162-71.
27. Akbari OA, Afrouzi HH, Marzban A, Toghraie D, Malekzade H, Arabpour A. Investigation of volume fraction of nanoparticles effect and aspect ratio of the twisted tape in the tube. *Journal of Thermal Analysis and Calorimetry*. 2017;129(3):1911-22.

28. Maddah H, Alizadeh M, Ghasemi N, Alwi SRW. Experimental study of Al<sub>2</sub>O<sub>3</sub>/water nanofluid turbulent heat transfer enhancement in the horizontal double pipes fitted with modified twisted tapes. *International Journal of Heat and Mass Transfer*. 2014;78:1042-54.
29. Torabi M, Zhang K, Karimi N, Peterson G. Entropy generation in thermal systems with solid structures—a concise review. *International Journal of Heat and Mass Transfer*. 2016;97:917-31.
30. Torabi M, Karimi N, Peterson G, Yee S. Challenges and progress on the modelling of entropy generation in porous media: a review. *International Journal of Heat and Mass Transfer*. 2017;114:31-46.
31. Shamsabadi H, Rashidi S, Esfahani JA. Entropy generation analysis for nanofluid flow inside a duct equipped with porous baffles. *Journal of Thermal Analysis and Calorimetry*. 2019;135(2):1009-19.
32. Ellahi R, Hassan M, Zeeshan A. Shape effects of nanosize particles in Cu–H<sub>2</sub>O nanofluid on entropy generation. *International Journal of Heat and Mass Transfer*. 2015;81:449-56.
33. Sroysroy A, Eiamsa-ard S. Enhancing convective heat transfer in laminar and turbulent flow regions using multi-channel twisted tape inserts. *International Journal of Thermal Sciences*. 2017;121:55-74.
34. Brinkman H. The viscosity of concentrated suspensions and solutions. *The Journal of Chemical Physics*. 1952;20(4):571-.
35. Maxwell JC, Thompson JJ. *A treatise on electricity and magnetism*. Clarendon; 1904.
36. Bejan A. *Entropy generation minimization: the method of thermodynamic optimization of finite-size systems and finite-time processes*. CRC press; 2013.

37. Manglik RM, Bergles AE. Heat transfer and pressure drop correlations for twisted-tape inserts in isothermal tubes: Part II—Transition and turbulent flows. *Journal of Heat Transfer*. 1993;115(4):890-6.
38. Nakhchi M, Esfahani J. CFD approach for two-phase CuO nanofluid flow through heat exchangers enhanced by double perforated louvered strip insert. *Powder Technology*. 2020; 877-88.